PRIFYSGOL
ABERYSTWYTH
UNIVERSITY

Aberystwyth University

1   **Knickpoint evolution in a supraglacial stream**

2   Kamintzis, J.E. [1]*, Irvine-Fynn, T.D.L.[1], Holt, T.O. [1], Jones, J.P.P. [2], Tooth, S.[1],

3   Griffiths, H.[1] and Hubbard, B.[1]

4   *[1]Department of Geography and Earth Sciences, Aberystwyth University, Aberystwyth, SY23*

5   *3DB, Wales, UK.*

6   *[2]Deri Jones & Associates, Ltd., Llwyngwyn, Forge, Machynlleth, SY20 8RR, Wales, UK.*

7

8   * Email: jek12@aber.ac.uk

9

10   Tristram David Linton Irvine-Fynn – tdi@aber.ac.uk, 01970622784, ORCiD: http://orcid.org/0000-

11   0003-3157-6646

12   Thomas Owen Holt – toh08@aber.ac.uk, 01970628449, ORCiD: https://orcid.org/0000-0001-8361-

13   0688, @tom_holt

14   John Paul Pryderi Jones – deri@djaweb.co.uk, 01654702001, @deri_jones

15   Stephen Tooth – set@aber.ac.uk, 01970622361, ORCiD: https://orcid.org/0000-0001-5714-2606

16   Hywel Griffiths – hmg@aber.ac.uk, 09170622674, ORCiD: https://orcid.org/0000-0002-0480-2014,

17   @HywelGriffiths

18   Bryn Hubbard – byh@aber.ac.uk, 01970622783, ORCiD: https://orcid.org/0000-0002-3565-3875,

19   @Bryn_Hubbard

20

21   Word count – 9426

22

23

24

25

26 **Knickpoint evolution in a supraglacial stream**

27 Despite numerous studies of knickpoints in bedrock and alluvial channels, no detailed
28 description of knickpoint change on ice has been reported to date. This paper presents
29 the first investigation of knickpoint evolution within a supraglacial stream. Repeat
30 longitudinal profile surveys of a knickpoint on Vadrec del Forno, Switzerland reveal a
31 step height increase of 115 mm and upstream migration of 0.26 m over three days during
32 the 2017 ablation season. Rates and magnitudes of erosion vary spatially across the
33 knickpoint in relation to differing discharge regimes. At high discharges (~ 0.013 m^3 s^{-1}),
34 erosion is focused at the step base; at low discharges (~ 0.003 m^3 s^{-1}), erosion is focused
35 on the reach upstream of the knickpoint, at the step lip and the step-riser face. This results
36 in replacement of knickpoint morphology, driven by frictional thermal erosion and
37 hydraulic action. Pool formation further influences step morphology, inducing secondary
38 circulation and increased melt at the base of the step-riser, causing steepening. Results
39 highlight the complexities of water flow over knickpoints, demonstrating that the stream
40 power law does not accurately characterise changing knickpoint morphology or predict
41 retreat rates. Although morphological similarities have been reported between
42 supraglacial and bedrock/alluvial channels, knickpoints in non-ice-walled channels will
43 not necessarily respond to discharge similarly to those in ice due to the different erosion
44 processes involved.

45 Keywords: knickpoint; step; supraglacial; evolution; hydrodynamics; discharge

1. Introduction

47 Knickpoints are commonly observed features in the longitudinal profile of river channel

48 systems. The term 'knickpoint' refers to channel reaches that exhibit a marked change in bed

49 slope, and is used herein to refer to an individual step, comprising the local point of abrupt

50 gradient change (the step lip) and the downstream channel-spanning steep segment (the 'step‑

51 riser'; Chartrand and Whiting 2000). Such changes in slope have been attributed to alterations

52 in sediment supply (Brush and Wolman 1960) and base-level change resulting from eustatic,

53 geological or tectonic perturbations (Haviv et al. 2010), with their presence increasing

54 hydraulic resistance and dissipating energy (Leopold et al. 1960; Abrahams et al. 1995; Curran

55 and Wohl 2003; Wilcox et al. 2011). Most knickpoints undergo upstream migration, governing

56 wider landscape changes through alteration of hillslope base level (Tucker and Whipple 2002;

57 Bigi et al. 2006; Whittaker and Boulton 2012). Three types of knickpoint retreat have been

58 identified by Gardner (1983) using flume experiments in cohesive, homogenous substrates: (i)

59 *parallel retreat* with retention of the original step morphology; (ii) *replacement* with alteration

60 of the original step morphology arising from erosion above the knickpoint lip and over the step

61 face; and (iii) *backward rotation* of the step towards the general channel slope, causing the

62 step-riser inclination to decrease. As adjustments in bedrock/alluvial channels typically occur

63 over decadal-to-millennial timescales, direct observations of upstream knickpoint retreat are

64 limited. Attempts have been made to predict knickpoint retreat rates in some landscapes using

65 the stream power incision model (Bishop et al. 2005; Crosby and Whipple 2006; Berlin and

66 Anderson 2007; Lague 2014). This model relates knickpoint retreat rate to catchment drainage

67 size, which acts as a proxy for discharge (Whipple and Tucker 1999; Crosby and Whipple

68 2006), assuming a constant flow regime. The stream power model, however, typically fails to

69 predict observations of knickpoint retreat due to poor characterisation of changing flow

70 regimes over a step (Dust and Wohl 2012), and the lack of consideration of sediment transport

71 processes (Jansen et al. 2011), the role of bedrock structure (Mackey et al. 2014), plunge-pool

72 dynamics (Scheingross and Lamb 2017) and the self-regulation of channel geometry (Baynes

73 et al. 2018).

74 Within bedrock channels, there is a lack of empirical data describing actively migrating

75 knickpoints (Cook et al. 2013), due to the typically slow retreat rates and difficulties in

76 identifying and isolating controlling intrinsic and extrinsic factors (Kephart 2013). Knickpoint

77 evolution mechanisms, therefore, remain poorly understood despite laboratory and flume

78 studies investigating drivers of change (e.g. Bennet et al. 2000; Grimaud et al. 2015; Lamb et

79 al. 2015; Baynes et al. 2018). However, knickpoint features have also been described in

80 supraglacial (e.g. Knighton 1981, 1985; Carver et al. 1994; St Germain and Moorman 2016)

and englacial channels (e.g. Pulina 1984; Holmlund 1988; Griselin 1992; Vatne 2001; Piccini et al. 2002; Vatne and Refsnes 2003; Vatne and Irvine-Fynn 2016), where their formation is considered to be related to intrinsic flow dynamics, in contrast to extrinsic factors commonly cited for bedrock/alluvial systems (Phillips et al. 2010; Yokokawa et al. 2016). This gives rise to a unique field environment that allows for isolation of hydrodynamic variables, since ice-walled streams are typically devoid of sediment load (Leopold et al. 1960; Kostrzewski and Zwoliñski 1995; Karlstrom et al. 2013), and channel boundaries are close to the melting point. These factors enable assessment of knickpoint evolution over shorter (hourly-to-diurnal) timescales. Supraglacial streams are often considered to be analogous to bedrock channels, due to their similarities in morphology and adjustment (Ewing 1970; Marston 1983; Knighton 1985; Karlstrom et al. 2013) and, thus, supraglacial investigations have been used to gain a better empirical understanding of channel formation and evolution (Ferguson 1973). Constraining supraglacial knickpoint evolution also has implications for understanding englacial drainage systems, at least where conduits exist at atmospheric pressure, owing to knickpoints forming a major component of vertical channel incision (Gulley et al. 2009; Vatne and Irvine-Fynn 2016) and, thereby, underpinning meltwater transfer to a glacier's ice-bed interface.

Currently, the potential of the supraglacial environment for examining knickpoint formation and evolution processes has not yet been fulfilled. The majority of field-based research on supraglacial streams was published several decades ago (e.g. Ewing 1970; Pinchack 1972; Dozier 1974; Hambrey 1977), and focused on hydraulic geometry (e.g. Park 1981; Marston 1983; Kostrzewski and Zwoliñski 1995; Brykała 1999) or meandering (e.g. Knighton 1972; Ferguson 1973). Although the presence of knickpoints has been reported (Dozier 1974), the only study to address this morphology in any detail examined its role in inducing pulsating flow (St Germain and Moorman 2016). Despite a recent resurgence of

interest in supraglacial drainage, studies have predominantly used remotely sensed data (e.g.
Joughin et al. 2013; Lampkin and VanderBerg 2014; Rippin et al. 2015; Smith et al. 2015;
Karlstrom and Yang 2016; Yang et al. 2016) and, thus, do not account for a process-level
understanding of local hydraulics. Therefore, there is a need to elucidate the processes
responsible for morphological drainage evolution through field-based research (Gleason et al.
2016), and to advance existing numerical models (e.g. Karlstrom et al. 2013; Mantelli et al.
2015).

Here, we present repeat geometric measurements of a knickpoint within a supraglacial
stream on Vadrec del Forno, Switzerland, to characterise its morphological evolution in
response to hydrodynamic forcing. Measurement took place over three days during the 2017
ablation season. The results provide the first description and quantification of changing
knickpoint morphology on ice, and yield insight into the varying spatial focus of hydrological
erosion at differing discharges.

2. Field site

Vadrec del Forno is a 4.5 km long, temperate, Alpine valley glacier located in the Bregaglia
Range of Graubünden, southeast Switzerland (46°17'N, 9°40'E; Figure 1A). The glacier flows
north from the Italian border, comprising two accumulation basins that form a shallow gradient,
~ 500 m wide tongue. The glacier elevation extended from ~ 2250 to 3200 m.a.s.l in 2016,
covering an area of 5 km^2. Across the ablation area, the predominant structural glaciological
feature is longitudinal foliation (Jennings et al. 2014), exerting a strong control over surface
meltwater drainage (cf. Hambrey 1977). This gives rise to relatively straight rills and streams
flowing parallel to the glacier flow direction, providing an excellent site for examining
hydrodynamics in straight channels unaffected by meander-induced secondary water
circulation.

2.1   Channel reach and knickpoint characteristics

A straight 4.5 m long reach of a perennial stream containing a single transverse knickpoint was

selected for investigation on the west side of the ablation zone, ~ 0.85 km from the terminus

(Figure 1). Glaciologically, perennial streams are channels that persist and are repeatedly

reoccupied over inter-annual timescales, in contrast to annual streams that form and melt out

each year (Ewing 1970). Perennial streams, especially on non-temperate glaciers, can seed the

formation of englacial channels existing at atmospheric pressure (Gulley et al. 2009), therefore,

providing a better analogue for englacial drainage than annual streams. Here, the selected reach

was chosen for the presence of a knickpoint in isolation, with the absence of any distinct

elevation changes that may have influenced knickpoint evolution. This stream was a

distributary, bifurcating from a main channel 9 m above the reach, and appeared to exploit the

downglacier oriented longitudinal foliation. The reach had a low gradient (7°) and sinuosity

(1.005), and ranged in width from 0.14 to 0.66 m. Despite evidence of several transverse clear

ice bands cutting across the channel upstream of the knickpoint, there was negligible transverse

structural variability at, or downstream of the knickpoint, suggestive of a homogenous substrate

underlying the step itself, allowing patterns and rates of change to be attributed to

hydrodynamic variables. Although clastic debris was visible embedded in the channel bed

(Figure 1B), the stream flow was devoid of sediment bed load, with little to no transportation

of ice crystals over the measurement period.

The knickpoint was classified as a 'break-in-gradient' knickpoint type (after Haviv et

al. 2010), characterised by a gentle step lip and riser face with a channel-bed-supported sloping

jet (Figure 1C). Over the measurement period, this knickpoint accounted for between 15 and

32 % of the 0.68 m decrease in elevation along the longitudinal profile of the stream reach.

Initially, no pooling of water at the step base was observed; instead, a reverse bed slope was

154 recorded downstream of the knickpoint with detachment of flow from the channel bed and

155 water aeration at the downstream end of this reverse slope.

156   [Figure 1 near here]

157   **3. Methods**

158 Data was collected in the early ablation season, between, and inclusive of, the 6th and 9th July

159 2017. This short measurement period arose from considerable water flow reduction over the

160 knickpoint on the 9th July, as a result of upstream flow capture. Knickpoint and channel

161 cross-section measurements were completed between 08:00 and 12:00 before peak diurnal

162 discharge, with the exception of the 6th July when measurements were taken between 14:00

163 and 15:30 and excluded cross-section geometry. Using the assumption that peak discharge has

164 the greatest impact on changing channel morphology (Marston 1983; Carver et al. 1994),

165 geometric measurements are considered to reflect adjustments resulting from the previous

166 day's hydrodynamic forcing. Adjustment was assessed between each day's measurements,

167 giving three full days of change monitoring.

168 *3.1   Knickpoint and channel geometry*

169 To measure knickpoint geometry, the majority of water flow over the step was temporarily

170 diverted to the main channel upstream of the reach, using sealed water-filled bags stacked at

171 the distributary diffluence. Water flow was diverted for ~ 20 minutes each day between 08:50

172 and 09:30. Once achieved, the horizontal distance of the step lip from a fixed reference point

173 was measured to determine upstream knickpoint recession. Daily central longitudinal profiles

174 of the step-riser were recorded using a contour gauge shaping tool, similar to techniques used

175 for quantifying surface roughness (McCarroll and Nesje 1996). The gauge maintains the shape

176 of a surface once moulded to it, allowing for replication with a quantified accuracy of 11 mm.

177 Careful gauge positioning onto laminated millimetre graph paper enabled tracing of the

178 lowermost edge using a whiteboard marker pen, with nadir photography using a 14-mpx

179 Fujifilm Finepix JV200 digital camera allowing for extraction of profile coordinates. These

180 profile coordinates were digitally plotted at centimetre resolution, using a Bezier spline

181 interpolation to represent the step-riser (accurate to 5 mm).

182 Channel cross-section geometry was measured upstream and downstream of the

183 knickpoint lip, to quantify vertical incision (Figure 1). Measurements were conducted from

184 fixed reference points, established on the east stream bank. From these points, vertical depth

185 measurements to the nearest 10 mm were recorded at 0.1 m intervals across the channel,

186 relative to a taut tape measure anchored on the opposite bank. Vertical depth measurements

187 and the 0.1 m measurement intervals were trigonometrically corrected to a horizontal plane,

188 using the tape angle measured with a compass clinometer to $\pm$ 1°, with depth adjustment to the

189 daily glacier surface elevation. The inevitable tape sag led to an uncertainty (C_{catenary}) that

190 was quantified following Uren and Price (2005):

191
$$C_{\text{catenary}} = \frac{w^2 D^3 (cos2\theta)}{24T^2}$$

192 (Equation 1)

193 where w is weight per unit length of tape, D is tape length, θ is the vertical angle between

194 end-points and T is applied tension. Assuming modest tension of 10 N, (following Irvine-Fynn

195 et al. (2014a)), for a tape length of 1.8 m and weight per unit length of 0.18 N m^{-1}, the maximum

196 uncertainty was 1 mm. Within the horizontal plane, inevitable positional uncertainty in repeat

197 surveys arises from ablation at the fixed reference points; however, this error is acceptable here,

198 as cross-sections are not directly compared in absolute space.

199 Bank full stage is unlikely within perennial supraglacial streams, as their existence

200 depends on incision outpacing ablation, at least initially (Knighton 1981; Marston 1983).

201 Therefore, flow geometry dimensions of the 'active channel' (width, mean channel depth

202 below the ice surface) were derived using water height at the channel thalweg (stage) at 10:00.

203 This 'active channel' denotes the area that adjusts in relation to actively flowing water

204 (Osterkamp and Hedman 1977), providing the best approximation of channel dimensions when

205 the channel is most stable prior to peak discharge. Daily incision rates were determined using

206 the difference between mean cross-section depths.

207 ### 3.2   *Streamflow dynamics*

208 Stream discharge was measured at hourly intervals between 09:30 and 13:30. Following

209 Hudson and Fraser (2002), discharge (Q) was estimated using salt dilution gauging:

210

$$Q = \frac{k\,M}{(T_2 - T_1) \times (EC - EC_{bkgd})}$$

211

212 (Equation 2)

213 where M is mass of salt added in grams (here, 10 g pre-dissolved salt injected 11 m upstream

214 of the detection point); $T_2 - T_1$ is tracer passage duration in seconds; $EC - EC_{bkgd}$ is mean

215 electrical conductivity during the tracer passage, as measured with a REED SD-4307

216 conductivity meter (0.1 μS resolution, accurate to ± 2 % (REED 2015)); and k is the

217 temperature-corrected proportionality constant, calculated as 1.5909 for 0 °C. Over the

218 observed temperature range of $0.01 - 0.3$ °C, variation in k was less than 1 % and negligible

219 for discharge calculations. Measurements characterised the rising limb and beginning of the

220 falling limb of diurnal discharge and, thus, captured daily peak discharge between 11:30 and

221 12:30. An additional discharge reading was taken on the 6th July at 15:00, while it was not

222 possible to derive discharge on the 9th July, as flow was too low to measure.

223   Flow velocity along the reach was calculated from the salt tracer travel time over the

224   thalweg distance and, following Knighton (1998), used with measurements of stage and flow

225   width to calculate Froude and Reynolds numbers (Fr and Re, respectively). Daily maximum

226   stream power per unit length over the knickpoint was estimated using the mean step gradient

227   and peak discharge. Detailed observations were also made regarding the nature of water flow

228   over the knickpoint, including defining the contact between the water and step-riser and

229   evidence of hydraulic jumps, backpooling and splashing of water in relation to the channel

230   morphology.

231   *3.3   Meteorological data*

232   In the absence of meteorological data at the glacier surface, hourly air temperature data over

233   the measurement period were obtained from the nearest MeteoSwiss automatic weather station,

234   located in Vicosoprano, 7 km from Vadrec del Forno. To interpolate these data to the local air

235   temperature at the study site, a relationship describing the lapse rate between Vicosoprano and

236   Vadrec del Forno was used, based on data from a HOBOware® weather station that had been

237   installed on the ice during July 2016. The calculated lapse rate ($r^2 = 0.72$, $p \leq 0.01$)

238   was -0.009 °C m^{-1}, giving a difference of 10.85 °C between the sites that was used to adjust the

239   2017 air temperature data. Hourly potential incident radiation at the glacier surface was

240   calculated following Irvine-Fynn et al. (2014b).

241   **4. Results**

242   *4.1   Knickpoint evolution*

243   The step lip migrated upstream by 0.26 m over three days from its initial 6th July position

244   (Figure 2), with the step-riser face steepening by 17°. Knickpoint recession rates were variable,

245   increasing from 0.01 m day^{-1} (6th - 7th July) to 0.08 m day^{-1} (7th - 8th July), with the greatest

246 recession of 0.17 m day^{-1} occurring between the 8th and 9th July, coincident with the greatest

247 change in step gradient (Table 1).

248   Step height increased by 115 mm with the greatest change of 88 mm occurring between

249 the 7th and 8th July. Between the 8th and 9th July, step height decreased by 18 mm. The reverse

250 bed slope at the step base was replaced with the formation of a pool towards midday on the 8th

251 July, with evidence of a hydraulic jump and backpooling.

252   [Figure 2 near here]

253   [Table 1 near here]

254 ***4.2   Cross-section evolution***

255 Measured cross-sections (Figure 3) show that above the knickpoint, the channel was generally

256 wider and shallower than below the knickpoint. Over the measurement period, mean channel

257 depth above the knickpoint was 0.40 m, and 0.52 m below the knickpoint. The nature and rates

258 of morphological change were variable over both space and time, with disparity between the

259 cross-sections. Above the knickpoint, the channel cross-section was initially approximately

260 trapezoidal (Figure 3A; 7th July). This cross-section incised by 27 mm, developing a more

261 rounded, quasi-elliptical morphology (Figure 3A; 8th July), which further incised by 83 mm

262 and narrowed by 160 mm to form a more triangular morphology (Figure 3A; 9th July). Below

263 the knickpoint (Figure 3B), the channel maintained an approximately triangular cross-section,

264 with a stable width (Table 1) and incision of 73 mm over the first two days (6th - 7th, 7th - 8th

265 July). This profile subsequently widened by 80 mm and incised by 20 mm (8th - 9th July).

266   The channel upstream of the knickpoint incised 18 mm more than that below, with the

267 majority of vertical incision occurring between the 8th and 9th July above the step, and between

268 the 7th and 8th July below the step (Table 1; cross-section mean depths). However, the greatest

269 change in width was recorded between the 8th and 9th July for both cross-sections. As a result,

270   deepening and narrowing of the upstream cross-section coincided with a decrease in incision

271   and widening of the downstream cross-section.

272   [Figure 3 near here]

273   ***4.3   Streamflow dynamics***

274   Over the measurement period, discharge generally decreased (Table 1), with peak discharge on

275   the 8th July being an order of magnitude lower than on previous days, and water flow on the 9th

276   July being too low to measure. Water temperatures correlated positively with discharge

277   ($r = 0.83$, n = 11, $p \leq 0.01$). Expectedly, discharge also correlated positively with velocity

278   ($r = 0.82$, n = 11, $p \leq 0.01$) and stream power ($r = 0.99$, n = 11, $p < 0.01$) and, thus, stream

279   power was significantly lower on the 8th July than on previous days ($p \leq 0.01$). The reduced

280   discharge (8th and 9th July) was the result of upstream water capture, due to the main channel

281   incising at a faster rate than the studied distributary reach. However, linear regressions between

282   discharge and stream power with knickpoint retreat were not significant ($p > 0.05$).

283   Water flow over the knickpoint was continuously channel-bed-supported, with only

284   occasional observations of decoupled flow for a few seconds at a time. Water flow above and

285   below the knickpoint was mainly subcritical (Fr < 1) and was predominantly turbulent on the

286   6th and 7th July (high Re), with transitional flow on the 8th July (Table 1). As water neared the

287   step base, lateral flow interaction with the channel banks resulted in water being diverted

288   upwards and back towards the channel centre, causing flow convergence here and at the

289   beginning of the reverse bed slope. A submerged impinging jet was observed at the step base.

290   Downstream of the knickpoint, flow detachment from the channel bed occurred as the reverse

291   bed slope deflected water upward, causing visible aeration and spraying of the channel banks.

292   Immediately prior to midday on the 8th July, the effects of the reverse bed slope were less

293   obvious and a hydraulic jump was present at the step base, with evidence of backpooling.

294   **5. Discussion**

295   *5.1   Hydrodynamic forcing*

296   In the absence of an appreciable bed load, it is reasonable to assume that erosive forces are

297   predominantly hydrodynamic, with hydraulic action and melting driving supraglacial channel

298   change (Knighton 1981; Marston 1983; Kostrzewski and Zwoliñski 1995; Isenko et al. 2005).

299   However, the results demonstrate that increased retreat rate was not associated with rising

300   discharge and stream power per unit length. This supports suggestions that the relationship

301   between discharge and knickpoint retreat rate is oversimplified (Baynes et al. 2018). Instead,

302   the results here show that greater knickpoint retreat occurred at lower discharges. The changing

303   step morphology indicates non-uniformity of erosion across the step, demonstrating the

304   complex interaction between discharge regime and knickpoint evolution (see Section 5.2).

305   Additionally, these data further demonstrate that the simplistic stream power incision model is

306   unlikely to adequately characterise retreating knickpoints (Howard et al. 1994; Scheingross

307   and Lamb 2017). This supports the work of St Germain and Moorman (2016), which

308   demonstrated that supraglacial step-pool morphologies do not necessarily form at high

309   discharge, contrary to assumptions by Vatne and Refsnes (2003) who regard high discharge as

310   a necessary factor for step formation in ice. Furthermore, this challenges the assumption that

311   the greatest channel change occurs at peak discharges in ice-walled channels (Marston 1983;

312   Carver et al. 1994), highlighting the need for measurements at increased temporal resolution to

313   better constrain the timing and rates of evolution.

314   As erosion reflects the balance between driving and resisting forces (Wohl 1998;

315   Hayakawa and Matsukura 2003), the role of ice substrate resistance in controlling knickpoint

316   migration rates must also be considered. The channel substrate comprised clear and bubbly ice

317   types, the former of which experiences preferential water erosion (Ewing 1970; Hambrey

318   1977), as exemplified by the undulating bed form troughs concordant with clear ice structures

319   upstream of the knickpoint (Figure 1B). The observed alternation in ice types through these

320   bed forms, had they extended downstream, could have explained the relative stability of the

321   step lip between the 6th and 7th July, with the subsequent increase in retreat rate being the result

322   of headward migration through clear ice to less resistant, bubbly ice upstream. However, the

323   absence of such structural features proximate to the knickpoint indicated a homogenous

324   substrate here, reflected by knickpoint migration via replacement. This implies that knickpoint

325   evolution was not structurally controlled during the measurement period, supporting the

326   argument that hydrodynamic forcing plays the dominant role in governing supraglacial step

327   evolution.

328   Within an ice-walled channel, thermal erosion is an additional contributing driver of

329   knickpoint retreat. Such heat energy transfer arises from several sources: sensible air

330   temperature and solar radiation, friction at the water-ice interface and turbulence-induced

331   friction within the water (Ewing 1970; Ferguson 1973; Marston 1983). Additional erosion can

332   arise from direct channel bed ablation through shallow water columns (Holmes 1955; Dozier

333   1974). Although direct ablation may have been possible in this study, given the maximum

334   recorded water depth of 0.1 m, this is not supported by the insignificant linear regression

335   between daily mean potential incident radiation and incision rates ($r = 0.027$, $p > 0.05$). Using

336   the 'Enter method', a multiple linear regression ($R^2 = 0.62$) demonstrates that discharge was

337   the only significant predictor of water temperature ($r = 0.75$, $p < 0.05$). This indicates that

338   frictional heat generated from viscous flow dissipation is the main component of thermal

339   erosion in this study, supporting research by Ferguson (1973), Parker (1975) and Marston

340   (1983) who estimated that this can account for $50 - 75$ % of incision. The overall slope of the

341   stream reach here was $7°$, with that of the knickpoint face being a minimum of $18°$. As Pinchack

342   (1972) reported a requisite channel gradient of $11°$ to induce melt in a slightly wider stream

343   than reported here, this indicates that frictional heat potentially plays more of a role in erosion

344   locally, thereby contributing to knickpoint evolution.

345   *5.2   Hydrological controls on supraglacial knickpoint evolution*

346   The notion that knickpoint retreat rate is primarily controlled by discharge (Seidl and Dietrich

347   1992; Howard et al. 1994; Bishop et al. 2005) is challenged by the supraglacial stream data

348   presented here. The greatest step retreat, gradient change and rate of upstream incision

349   (Cross-section A) were associated with low discharges, and the greatest increase in step height

350   and rate of downstream incision (Cross-section B) were associated with high discharges. To

351   explain these spatial and temporal variations, we propose a conceptual model of

352   process-morphology linkages to identify the hydrological controls on supraglacial knickpoint

353   evolution, whereby varying discharge regimes control spatial zones of erosion over the

354   step-riser and lead to pool formation (Figure 4). Three morphologically distinct zones of

355   erosion are identified, with differential rates and magnitudes of change at the step lip, riser face

356   and step base giving rise to knickpoint evolution via replacement of step morphology (Gardner

357   1983).

358   At turbulent, high discharges, (here, 6th and 7th July), vertical incision is focused at the

359   step base. The reduced boundary resistance at high flows means that the impinging jet retains

360   energy over the step lip and face (Marston 1983; Wilcox and Wohl 2006; Comiti et al. 2009),

361   therefore, imparting greater hydraulic force to the step base. However, as the channel bed and

362   step face were not smoothly polished, channel roughness elements were limited to microscale

363   features, indicating that reduced boundary resistance is likely to have a negligible impact on

364   energy retention. At the step base, higher water temperatures associated with turbulence are

365   more likely to contribute to vertical incision, aided by the high degree of interaction between

366   the water jet and the channel bed. Incision rates at the step base exceed those at the lip, leading

367   to an increase in step height. Consequently, the knickpoint experiences considerable

368   steepening, which contradicts the more often observed backward rotation of the knickpoint in

369   homogenous bedrock and alluvial settings (Holland and Pickup 1976; Gardner 1983; Stein and

370   Julien 1993; Frankel et al. 2007).

371   [Figure 4 near here]

372   At low discharges with transitional flow, (here, 8th and 9th July), erosion is focused on

373   the reach immediately upstream of the knickpoint, the step lip and the step-riser face. At low

374   water depths, the microscale channel roughness has a greater influence on frictional energy

375   dissipation, increasing boundary resistance and resulting in accelerated melting of the bed

376   upstream of the step, and at the step lip where shear stress is highest (Gardner 1983). The lower

377   velocities associated with lower discharges act to increase the energy transfer time and, thus,

378   enhance melt at a given point (Thorsness and Hanratty 1979), with low turbulence inhibiting

379   energy dissipation within the flow itself. This occurs mainly above the step lip, where water

380   flow is slower than across the step-riser as a result of the gentler slope. Additionally, enhanced

381   erosion above the step lip is attributed to over-steepening (drawdown) of the water surface

382   profile as flow starts to accelerate over the increasing gradient (Gardner 1983; Haviv et al.

383   2006; Berlin and Anderson 2009). This enhanced energy transfer reduces the stream power of

384   the bed-supported jet (Chin 2003), resulting in less available energy to hydraulically erode the

385   step base and causing a decrease in step height.

386   The finding that low discharge has a dominant control on knickpoint migration

387   necessitates consideration of the potential methodological impact of temporary stream

388   diversion during low flows. The magnitude of knickpoint and channel adjustment was in the

389   order of centimetres to decimetres over 24 hours, with peak diurnal discharge only exceeding

390    $0.009 \ \mathrm{m^3 \, s^{-1}}$ for a maximum of 3.5 hours over the measurement period. Low flow conditions

391   of $< 0.007 \ \mathrm{m^3 \, s^{-1}}$ were recorded throughout the rest of the day, with flow diversion for 20

392 minutes accounting for < 2 % of this time, assuming continuous 24 hour flow. Consequently,

393 we suggest that flow diversion over such a short period had negligible impact on knickpoint

394 evolution; however, a portion of low flow channel adjustment may have been overlooked,

395 albeit small, as a result of this diversion. The estimated maximum discharge diverted to the

396 main channel (~ 0.005 $m^3 s^{-1}$) is not expected to have resulted in a marked change in incision

397 rate or eventual channel capture over the timescales involved.

398 *5.2.1   Hydrological controls on pool development*

399 The lack of ice structural control over observed knickpoint evolution suggests that downstream

400 pool development on the 8th July was primarily controlled by step morphology adjustment in

401 response to discharge variations. Using the conceptual model described in Figure 4, an

402 explanation for pool formation can be proposed. At high discharges, localised erosion at the

403 step base leads to over-deepening. Water pools in this depression at low discharges, with the

404 reverse bed slope acting to further impede downstream flow. As pool development starts to

405 reduce the effect of the impinging jet on the channel bed (Wu and Rajaratnam 1998;

406 Zimmermann and Church 2001; Carling et al. 2005), the increased tailwater depth inhibits

407 vertical incision and results in a predominance of lateral erosion. In our study, this is

408 demonstrated by the coincident decrease in channel depth and increase in width below the

409 knickpoint between the 8th and 9th July. The pooled water creates a persistent contact with the

410 ice forming the lower section of the step-riser, causing erosion here (Figure 4), and resulting in

411 continued and accelerated steepening of the face at low discharge. Turbulent secondary

412 circulation back towards the step face and the formation of a hydraulic jump close to the step

413 base enhances this erosional zone. Pool development herein appears to conform

414 morphologically to the conceptual model proposed by Scheingross et al. (2017) to describe

415 abrasive plunge-pool evolution in homogenous bedrock. This suggests that in a homogenous

416 ice substrate and, even in the absence of sediment load, knickpoint retreat may be driven by

417 vertical drilling, a knickpoint migration process described by Howard et al. (1994) and Lamb

418 et al. (2007). This contrasts with classic waterfall erosion models that indicate knickpoint

419 migration owing to overlying caprock failure, following removal of an underlying substrate

420 (e.g. Gilbert 1890; Holland and Pickup 1976; Frankel et al. 2007). However, the lack of

421 undercutting herein may be due to the reduced discharge following pool formation, with

422 accelerated erosion of the upstream pool wall only being plausible in the case of continued

423 flow.

424   Although substrate characteristics influence the shape and recession rate of knickpoints

425 (Gardner 1983; Larue 2008; Phillips and Desloges 2014), our proposed model builds on the

426 concept that a mutual interaction exists between the shape of the heat transfer surface and the

427 variation in rates of heat transfer, the latter of which is determined by flow characteristics

428 (Gilpin et al. 1980). This advances the work of Vatne and Irvine-Fynn (2016), whose insights

429 from englacial knickpoint morphology indicated that step shape controls the type of water jet

430 and, thus, the location of energy expenditure and heat transfer across the knickpoint face. Our

431 model demonstrates that differing discharge regimes govern the location of erosion, a concept

432 that can be extended to knickpoint evolution in bedrock (Carling et al. 2005) and cohesive

433 sediment (Bennet et al. 2000), where varying degrees of surface erosion in relation to

434 hydrological forcing have also been recorded. However, the difference in erosive mechanisms

435 between supraglacial and bedrock/alluvial channels indicates that this model is not applicable

436 within the latter for determining the ways in which knickpoint morphology will adjust in

437 response to discharge alterations. Contrary to some previous assertions (e.g. Ewing 1970;

438 Marston 1983; Knighton 1985), this shows that the systems are not analogous to one another,

439 warranting further investigation into the differences between each environment and the

440 processes causing the formation and adjustment of similar channel morphologies.

441 ### *5.3 Interactions between morphology and flow variability*

442 The zones of erosion outlined in Section 5.2 govern step and channel shape, and demonstrate

443 the effect of flow dynamics on knickpoint morphology. However, channel morphology also

444 controls flow dynamics over a step (e.g. Knighton 1981; Kostrzewski and Zwoliñski 1995;

445 Milzow et al. 2006), determining these erosional zones. Here, this is exemplified by channel

446 narrowing over the knickpoint, confining water flow over the step-riser and resulting in water

447 overturning towards the channel centre with consequent flow convergence. This, in turn, gives

448 rise to the narrow cross-section at the step base, with water concentration driving vertical

449 incision. This feedback between channel morphology and hydraulics is complex, making it

450 difficult to identify clear cause-and-effect relationships (Wilcox et al. 2011).

451 In order to determine the importance of the erosional zones outlined here in controlling

452 knickpoint morphology and recession rates, knickpoint evolution was modelled (Figure 5)

453 using the daily ice melt rate as an equivalent erosional process for the stream power incision

454 model. Channel incision rates were derived from daily mean water temperature and velocity,

455 using relationships described in Isenko et al. (2005)'s Figure 2. Each knickpoint profile was

456 divided into linear millimetre-to-centimetre length segments based on changes in gradient

457 using Rhino3D® software (Robert McNeel & Associates 2017), with application of calculated

458 daily incision rates perpendicular to the local slope of each segment. Perpendicular offsetting

459 of each segment reflected changes in the horizontal and vertical plane, and better characterised

460 knickpoint retreat and morphological adjustment. A manually digitised curve joined the offset

461 segments to create a full modelled profile (Figure 5). As discharge prior to 08:00 was

462 consistently low (< 0.005 m^3 s^{-1}), it is assumed that stream flow is also low in the evening and

463 negligible overnight. This assumption is supported by the high snow line position in July 2017,

464 akin to that typically seen in late summer (Beat Kühnis, personal communication, July 2017).

465 Snowpack depletion reduces potential water storage at the glacier surface, the volume of

466 delayed runoff and the lag-time between peak melt and supraglacial discharge (see Willis et al.

467 2002). Here, the contribution of delayed runoff following peak ablation is likely to be minimal,

468 indicating that the stream did not experience continuous water flow over a 24-hour period.

469 Therefore, incision rates were applied for an 18-hour period to represent a maximum estimate

470 of change, as the mean water temperatures and velocities used encompassed the rising limb

471 and peak diurnal measurements.

472 [Figure 5 near here]

473 Comparison of the modelled profiles with observed knickpoint evolution emphasise

474 discrepancies between both the shape and rate of evolution (Figure 5). Modelled profiles

475 retained the original step morphology, overestimating vertical lowering (6th - 7th, 8th - 9th July)

476 and both overestimating (6th - 7th July) and underestimating headward recession at the step lip

477 (7th - 8th, 8th - 9th July). The inability of the model to accurately predict knickpoint evolution on

478 ice is likely due to the assumption of constant water temperature and velocity along the profile.

479 As the results herein demonstrate that differential zones of erosion arise at differing discharges,

480 this suggests that use of a constant-rate melt model for characterising step evolution is too

481 simplistic, similar to the stream power laws applied in bedrock/alluvial streams. The

482 complexities of changing flow dynamics across a knickpoint on ice must be further

483 investigated, to allow incorporation of these parameters and their feedback with the channel

484 boundary into numerical models.

485 **6. Conclusions**

486 Until now, there has been a limited process-level understanding of knickpoint evolution within

487 ice-walled channels, despite their importance in supraglacial and englacial incision processes.

488 Our study of a supraglacial knickpoint on Vadrec del Forno, Switzerland provides the first

489 detailed dataset of supraglacial knickpoint morphological change at a fine temporal resolution.

490 The results showed recession of 0.26 m over three days, with variable rates and magnitudes of

491   change, both spatially across the knickpoint and temporally over diurnal timescales. Low flow

492   rates coincided with the greatest step retreat, gradient change and rate of upstream incision,

493   and high flow rates coincided with the greatest increase in step height and rate of downstream

494   incision. Our conceptual model proposes that discharge variations control the zones of erosion

495   over the knickpoint, with low discharge focusing erosion on the reach upstream of the

496   knickpoint, the step lip and step-riser face, and high discharge focusing erosion at the

497   knickpoint base. Channel over-deepening at the knickpoint base led to pool formation, with the

498   increased tailwater depth inhibiting vertical incision and causing lateral erosion. This confirms

499   non-uniform water flow over the step, resulting in evolution through replacement of

500   morphology. Bed load absence within the stream indicates the hydrodynamic nature of

501   evolution, with the driving forces of hydraulic action and frictional thermal erosion governing

502   morphological change. The results indicate that peak discharge may not play as dominant a

503   role in drainage development on ice as previously considered, suggesting that the majority of

504   morphological adjustment in features such as knickpoints may occur prior to or following high

505   meltwater fluxes, either at a diurnal (supraglacial) or seasonal (englacial) scale.

506   The data presented here demonstrate that the relationships between discharge, stream

507   power and knickpoint retreat rate commonly used in bedrock/alluvial channels fails to capture

508   the intricacies and feedbacks of erosion processes driving knickpoint recession in ice-walled

509   channels. Our findings show that the considerable differences in erosive mechanisms between

510   supraglacial and bedrock/alluvial channels are likely to result in disparities in knickpoint

511   morphological adjustment in response to varying discharge regimes. The conceptual model

512   proposed herein has been developed from a relatively time-limited dataset, meaning that

513   ascertaining whether results provide a relevant representation of knickpoint evolution is

514   challenging. In order to test the wider application of the model, additional research within

515   supraglacial environments is required at a range of spatial scales, taking into consideration

516 channels of varying sizes, gradients and discharges. In particular, further investigation of

517 knickpoint erosion mechanisms in relation to variable flow regimes is essential, through

518 increasing the *temporal* and *spatial* resolution of flow measurements above, across and below

519 knickpoints.

535 **Disclosure statement**

536 No potential conflict of interest was reported by the authors.

537 **Notes on contributors**

538 JEK is a PhD student in Glaciology at the Centre for Glaciology, Aberystwyth University. Her

539 main area of research is glacier drainage morphology.

540 TDLI-F is a Senior Lecturer in Geography at Aberystwyth University. His main area of

541 research is glacial hydrology, which includes the hydraulics of the near-surface ice, the

542 seasonal development of ice surface roughness and albedo, and glacier surface microbial

543 processes.

544 TOH is a Lecturer in Geography at Aberystwyth University, specialising in glaciology and

545 remote sensing. His research focuses on the use of optical, radar and microwave imagery and

546 data to quantify changes in the cryosphere.

547 JPPJ is an engineering consultant and surveyor specialising in marine design and laser scanning

548 for Deri Jones & Associates Ltd. His work focuses on the design of construction systems for

549 large structures, and on capturing 3D information for complex man-made and natural

550 structures.

551 ST is a Professor of Geography at Aberystwyth University. His main areas of research include

552 fluvial geomorphology and sedimentology, with a particular focus on bedrock and alluvial

553 rivers in drylands.

554 HMG is a Senior Lecturer in Geography at Aberystwyth University. His main areas of research

555 include processes and rates of change in fluvial systems and reconstructing flood histories using

556 geomorphological and documentary methods.

557 BH is a Professor of Geography at Aberystwyth University. His main areas of research include

558 the links between subglacial drainage and ice motion, structural glaciology and glacier-like

559 forms on Mars.

560 **Author contributions**

561 JEK and TDLI-F developed the research question and context; JEK designed and conducted

562 the research; JEK analysed and interpreted the data, and wrote the paper with guidance from

563 TDLI-F; TOH provided UAV imagery of the field site. All authors edited and revised the paper.

References

Abrahams AD, Li G, Atkinson JF. 1995. Step-pool streams: Adjustment to maximum flow resistance. Water Resour Res. 31(10):2593-2602.

Baynes ER, Lague D, Attal M, Gangloff A, Kirstein LA, Dugmore AJ. 2018. River self-organisation inhibits discharge control on waterfall migration. Sci Rep. 8(1):2444.

Bennet SJ, Robinson KM, Simon A, Hanson GJ. 2000. Stable knickpoints formed in cohesive sediment. Joint Conference on Water Resource Engineering and Water Resources Planning and Management; 30th July - August 2nd; Minneapolis, MN.

Berlin MM, Anderson RS. 2007. Modeling of knickpoint retreat on the Roan Plateau, western Colorado. J Geophys Res Earth Surf. 112(F3).

Berlin MM, Anderson RS. 2009. Steepened channels upstream of knickpoints: Controls on relict landscape response. J Geophys Res Earth Surf. 114(F03018).

Bigi A, Hasbargen LE, Montanari A, Paola C. 2006. Knickpoints and hillslope failures: Interactions in a steady-state experimental landscape. Special Papers Geological Society of America. 398:295-307.

Bishop P, Hoey TB, Jansen JD, Artza IL. 2005. Knickpoint recession rate and catchment area: the case of uplifted rivers in Eastern Scotland. Earth Surf Processes Landforms. 30(6):767-778.

Brush JLM, Wolman GM. 1960. Knickpoint behavior in noncohesive material: a laboratory study. Geol Soc Am Bull. 71(1):59-74.

Brykała D. 1999. Hydraulic geometry of a supraglacial stream on the Waldemar Glacier (Spitsbergen) in the summer of 1997. Polish Polar Studies: 26th International Polar Symposium; June 1999; Lublin, Poland. p. 51-64.

Carling P, Tych W, Richardson K. 2005. The hydraulic scaling of step-pool systems. River, Coastal and Estuarine Morphodynamics. New York: Taylor & Francis; p. 55-63.

Carver S, Sear D, Valentine E. 1994. An observation of roll waves in a supraglacial meltwater channel, Harlech Gletscher, East Greenland. J Glaciol. 40(134):75-78.

589   Chartrand SM, Whiting PJ. 2000. Alluvial architecture in headwater streams with special emphasis on
590   step-pool topography. Earth Surf Processes Landforms. 25(6):583-600.

591   Chin A. 2003. The geomorphic significance of step–pools in mountain streams. Geomorphology.
592   55(1-4):125-137.

593   Comiti F, Cadol D, Wohl EE. 2009. Flow regimes, bed morphology, and flow resistance in self-
594   formed step-pool channels. Water Resour Res. 45(4):W04424.

595   Cook KL, Turowski JM, Hovius N. 2013. A demonstration of the importance of bedload transport for
596   fluvial bedrock erosion and knickpoint propagation. Earth Surf Processes Landforms. 38(7):683-695.

597   Crosby BT, Whipple KX. 2006. Knickpoint initiation and distribution within fluvial networks: 236
598   waterfalls in the Waipaoa River, North Island, New Zealand. Geomorphology. 82(1-2):16-38.

599   Curran JH, Wohl EE. 2003. Large woody debris and flow resistance in step-pool channels, Cascade
600   Range, Washington. Geomorphology. 51(1-3):141-157.

601   Dozier J. 1974. Channel adjustments in supraglacial streams. Icefield Ranges Research Project,
602   Scientific Results. 4:189-205.

603   Dust D, Wohl E. 2012. Characterization of the hydraulics at natural step crests in step-pool streams
604   via weir flow concepts. Water Resour Res. 48(W09542).

605   Ewing KJ. 1970. Supraglacial streams on the Kaskawulsh Glacier, Yukon Territory. Arctic Institute of
606   North America Research paper. 57:121-167.

607   Ferguson RI. 1973. Sinuosity of supraglacial streams. Geol Soc Am Bull. 84(1):251-256.

608   Frankel KL, Pazzaglia FJ, Vaughn JD. 2007. Knickpoint evolution in a vertically bedded substrate,
609   upstream-dipping terraces, and Atlantic slope bedrock channels. Geol Soc Am Bull. 119(3-4):476-
610   486.

611   Gardner TW. 1983. Experimental study of knickpoint and longitudinal profile evolution in cohesive,
612   homogenous material. Geol Soc Am Bull. 94(5):664-672.

613   Gilbert G. 1890. The history of the Niagara River: extracted from the sixth annual report to the
614   Commissioners of the State Reservation at Niagara, for the year 1889. Albany, NY.

615   Gilpin R, Hirata T, Cheng K. 1980. Wave formation and heat transfer at an ice-water interface in the
616   presence of a turbulent flow. J Fluid Mech. 99(3):619-640.

617   Gleason CJ, Smith LC, Chu VW, Legleiter CJ, Pitcher LH, Overstreet BT, Rennermalm AK, Forster
618   RR, Yang K. 2016. Characterizing supraglacial meltwater channel hydraulics on the Greenland Ice
619   Sheet from in situ observations. Earth Surf Processes Landforms. 41(14):2111-2122.

620   Grimaud J-L, Paola C, Voller V. 2015. Experimental migration of knickpoints: influence of style of
621   base-level fall and bed lithology. Earth Surf Dyn. 3(3):11-23.

622   Griselin M. 1992. In the depth of a small polar glacier (Loven East Glacier, Spitsbergen). Proceedings
623   of the 2nd International GLACKIPR Symposium; 10-16 February; University of Silesia, Poland. p.
624   51-63.

625   Gulley JD, Benn DI, Müller D, Luckman A. 2009. A cut-and-closure origin for englacial conduits in
626   uncrevassed regions of polythermal glaciers. J Glaciol. 55(189):66-80.

627   Hambrey MJ. 1977. Supraglacial drainage and its relationship to structure, with particular reference to
628   Charles Rabots Bre, Okstindan, Norway. Norsk Geografisk Tidsskrift. 31(2):69-77.

629   Haviv I, Enzel Y, Whipple K, Zilberman E, Matmon A, Stone J, Fifield K. 2010. Evolution of vertical
630   knickpoints (waterfalls) with resistant caprock: Insights from numerical modeling. J Geophys Res F:
631   Earth Surf. 115(F03028).

632   Haviv I, Enzel Y, Whipple KX, Zilberman E, Stone J, Matmon A, Fifield LK. 2006. Amplified
633   erosion above waterfalls and oversteepened bedrock reaches. J Geophys Res F: Earth Surf.
634   111(F04004).

635   Hayakawa Y, Matsukura Y. 2003. Recession rates of waterfalls in Boso Peninsula, Japan, and a
636   predictive equation. Earth Surf Processes Landforms. 28(6):675-684.

637   Holland W, Pickup G. 1976. Flume study of knickpoint development in stratified sediment. Geol Soc
638   Am Bull. 87(1):76-82.

639 Holmes GW. 1955. Morphology and hydrology of the Mint Julep area, Southwest Greenland.

640 Alabama, US: Air University. Mint Julep Reports., Part II: A-104-B.

641 Holmlund P. 1988. Internal geometry and evolution of moulins, Storglaciären, Sweden. J Glaciol.

642 34(117):242-248.

643 Howard AD, Dietrich WE, Seidl MA. 1994. Modeling fluvial erosion on regional to continental

644 scales. J Geophys Res B: Solid Earth. 99(B7):13971-13986.

645 Hudson R, Fraser J. 2002. Alternative methods of flow rating in small coastal streams. BC, Canada:

646 Forest Service British Columbia. EN-014.

647 Irvine-Fynn TDL, Sanz-Ablanedo E, Rutter N, Smith MW, Chandler JH. 2014a. Measuring glacier

648 surface roughness using plot-scale, close-range digital photogrammetry. J Glaciol. 60(223):957-969.

649 Irvine-Fynn TDL, Hanna E, Barrand N, Porter P, Kohler J, Hodson A. 2014b. Examination of a

650 physically based, high-resolution, distributed Arctic temperature-index melt model, on Midtre

651 Lovénbreen, Svalbard. Hydrol Processes. 28(1):134-149.

652 Isenko E, Naruse R, Mavlyudov B. 2005. Water temperature in englacial and supraglacial channels:

653 Change along the flow and contribution to ice melting on the channel wall. Cold Reg Sci Technol.

654 42(1):53-62.

655 Jansen JD, Fabel D, Bishop P, Xu S, Schnabel C, Codilean AT. 2011. Does decreasing paraglacial

656 sediment supply slow knickpoint retreat? Geology. 39(6):543-546.

657 Jennings SJ, Hambrey MJ, Glasser NF. 2014. Ice flow-unit influence on glacier structure, debris

658 entrainment and transport. Earth Surf Processes Landforms. 39(10):1279-1292.

659 Joughin I, Das SB, Flowers G, Behn MD, Alley RB, King MA, Smith B, Bamber JL, van den Broeke

660 MR, Van Angelen J. 2013. Influence of ice-sheet geometry and supraglacial lakes on seasonal ice-

661 flow variability. The Cryosphere. 7(4):1185-1192.

662 Karlstrom L, Gajjar P, Manga M. 2013. Meander formation in supraglacial streams. J Geophys Res

663 Earth Surf. 118(3):1897-1907.

664   Karlstrom L, Yang K. 2016. Fluvial supraglacial landscape evolution on the Greenland Ice Sheet.
665   Geophys Res Lett. 43(6):2683-2692.

666   Kephart CW. 2013. Flow and geometry measurements at an active knickpoint [Master's thesis].
667   Lincoln: University of Nebraska.

668   Knighton AD. 1972. Meandering habit of supraglacial streams. Geol Soc Am Bull. 83(1):201-204.

669   Knighton AD. 1981. Channel form and flow characteristics of supraglacial streams, Austre
670   Okstindbreen, Norway. Arct Alp Res. 13(3):295-306.

671   Knighton AD. 1985. Channel form adjustment in supraglacial streams, Austre Okstindbreen, Norway.
672   Arct Alp Res. 17(4):451-466.

673   Knighton AD. 1998. Fluvial Forms and Processes. London: Hodder Arnold.

674   Kostrzewski A, Zwoliñski Z. 1995. Hydraulic geometry of a supraglacial stream. Quaestiones
675   Geographicae. [accessed 11/05/2018]:[165-176 p.]. http://www.staff.amu.edu.pl/~zbzw/gh/gh1.htm.

676   Lague D. 2014. The stream power river incision model: evidence, theory and beyond. Earth Surf
677   Processes Landforms. 39(1):38-61.

678   Lamb MP, Finnegan NJ, Scheingross JS, Sklar LS. 2015. New insights into the mechanics of fluvial
679   bedrock erosion through flume experiments and theory. Geomorphology. 244:33-55.

680   Lamb MP, Howard AD, Dietrich WE, Perron JT. 2007. Formation of amphitheater-headed valleys by
681   waterfall erosion after large-scale slumping on Hawai'i. Geol Soc Am Bull. 119(7-8):805-822.

682   Lampkin D, VanderBerg J. 2014. Supraglacial melt channel networks in the Jakobshavn Isbræ region
683   during the 2007 melt season. Hydrol Processes. 28(25):6038-6053.

684   Larue J-P. 2008. Effects of tectonics and lithology on long profiles of 16 rivers of the southern Central
685   Massif border between the Aude and the Orb (France). Geomorphology. 93(3-4):343-367.

686   Leopold LB, Bagnold RA, Wolman MG, Brush JLM. 1960. Flow resistance in sinuous or irregular
687   channels. Washington, D.C.: Geological Survey Professional Paper. 282-D:111.

688   Mackey BH, Scheingross JS, Lamb MP, Farley KA. 2014. Knickpoint formation, rapid propagation,

689   and landscape response following coastal cliff retreat at the last interglacial sea-level highstand:

690   Kaua'i, Hawai'i. Geol Soc Am Bull. 126(7-8):925-942.

691   Mantelli E, Camporeale C, Ridolfi L. 2015. Supraglacial channel inception: Modeling and processes.

692   Water Resour Res. 51(9):7044-7063.

693   Marston RA. 1983. Supraglacial stream dynamics on the Juneau Icefield. Ann Assoc Am Geogr.

694   73(4):597-608.

695   McCarroll D, Nesje A. 1996. Rock surface roughness as an indicator of degree of rock surface

696   weathering. Earth Surf Processes Landforms. 21(10):963-977.

697   Milzow C, Molnar P, McArdell BW, Burlando P. 2006. Spatial organization in the step-pool structure

698   of a steep mountain stream (Vogelbach, Switzerland). Water Resour Res. 42(W04418).

699   Osterkamp W, Hedman E. 1977. Variation of width and discharge for natural high-gradient stream

700   channels. Water Resour Res. 13(2):256-258.

701   Park CC. 1981. Hydraulic geometry of a supraglacial stream: some observations from the Val

702   d'herens, Switzerland. Revue de Géomorphologie Dynamique. 30(1):1-9.

703   Parker G. 1975. Meandering of supraglacial melt streams. Water Resour Res. 11(4):551-552.

704   Phillips JD, McCormack S, Duan J, Russo JP, Schumacher AM, Tripathi GN, Brockman RB, Mays

705   AB, Pulugurtha S. 2010. Origin and interpretation of knickpoints in the Big South Fork River basin,

706   Kentucky–Tennessee. Geomorphology. 114(3):188-198.

707   Phillips R, Desloges J. 2014. Glacially conditioned specific stream powers in low-relief river

708   catchments of the southern Laurentian Great Lakes. Geomorphology. 206:271-287.

709   Piccini L, Romeo A, Badino G. 2002. Moulins and marginal contact caves in the Gornergletscher,

710   Switzerland. Nimbus. 23-24:94-99.

711   Pinchack AC. 1972. Diurnal flow variations and thermal erosion in supraglacial streams. East

712   Lansing, Michigan: Michigan State University. Technical Report 33: Part XII.
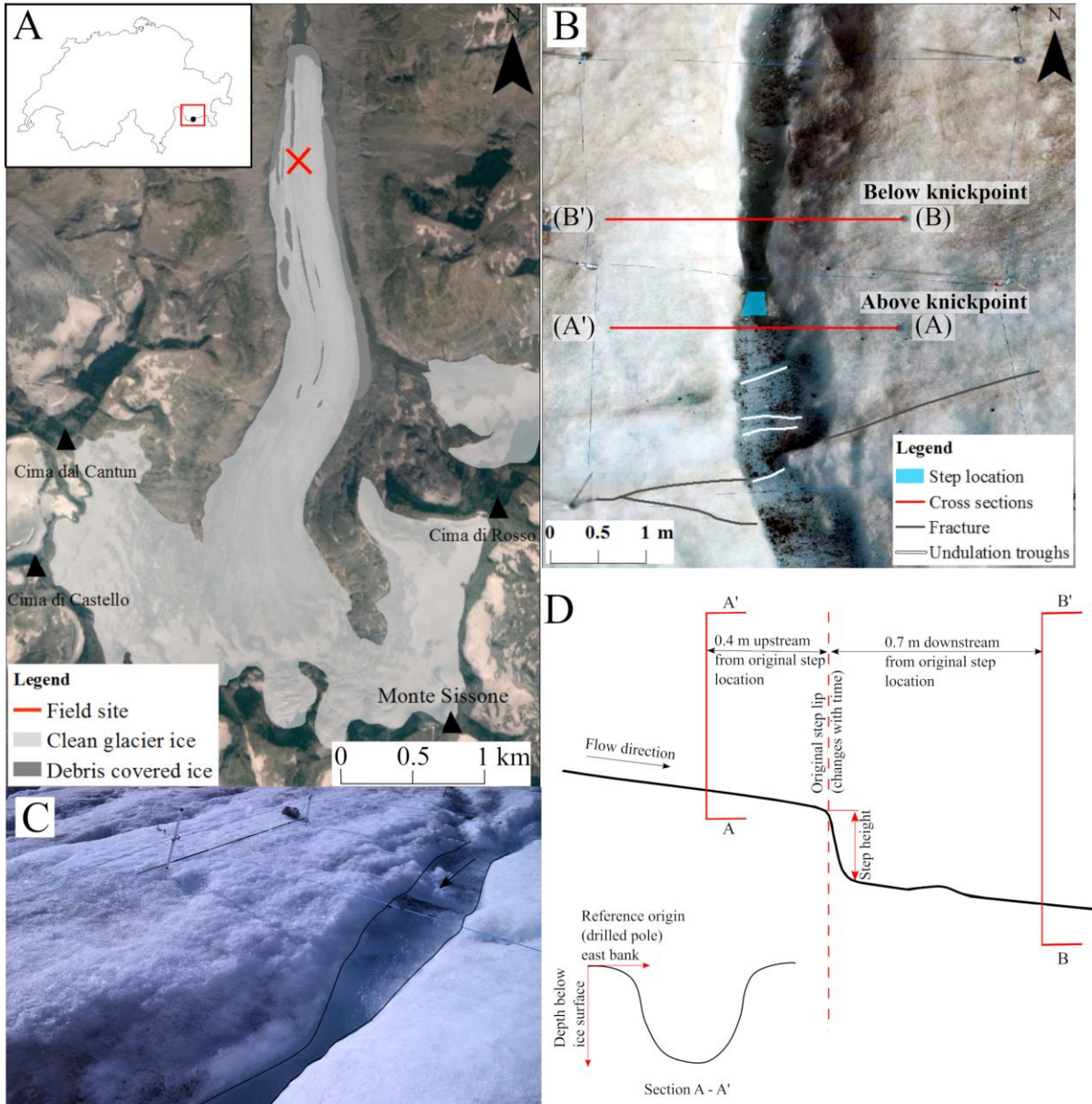
713   PlanetTeam. 2017. Planet Application Program Interface: In Space for Life on Earth. San Francisco,
714   CA.

715   Pulina M. 1984. Glacierkarst phenomena in Spitsbergen. Norsk Geografisk Tidsskrift. 38(3-4):163-
716   168.

717   REED Instruments. 2015. REED SD-4307 Salt/TDS/Conductivity Datalogger Instruction Manual.
718   REED Instruments.

719   Rippin DM, Pomfret A, King N. 2015. High resolution mapping of supra-glacial drainage pathways
720   reveals link between micro-channel drainage density, surface roughness and surface reflectance. Earth
721   Surf Processes Landforms. 40(10):1279-1290.

722   Robert McNeel & Associates. 2017. Rhino3D software Version 5. Barcelona: Robert McNeel &
723   Associates.

724   Scheingross JS, Lamb MP. 2017. A mechanistic model of waterfall plunge pool erosion into bedrock.
725   J Geophys Res F: Earth Surf. 122(11):2079-2104.

726   Scheingross JS, Lo DY, Lamb MP. 2017. Self-formed waterfall plunge pools in homogeneous rock.
727   Geophys Res Lett. 44(1):200-208.

728   Seidl M, Dietrich W. 1992. The problem of bedrock channel erosion. Catena Supplement. 23:101-
729   124.

730   Smith LC, Chu VW, Yang K, Gleason CJ, Pitcher LH, Rennermalm AK, Legleiter CJ, Behar AE,
731   Overstreet BT, Moustafa SE. 2015. Efficient meltwater drainage through supraglacial streams and
732   rivers on the southwest Greenland Ice Sheet. Proc Natl Acad Sci USA. 112(4):1001-1006.

733   St Germain S, Moorman B. 2016. The development of a pulsating supraglacial stream. Ann Glaciol.
734   57(72):31-38.

735   Stein O, Julien P. 1993. Criterion delineating the mode of headcut migration. J Hydraul Eng.
736   119(1):37-50.

737   Thorsness C, Hanratty T. 1979. Mass-transfer between a flowing fluid and a solid wavy surface.
738   AIChE Journal. 25(4):686-697.

739   Tucker G, Whipple K. 2002. Topographic outcomes predicted by stream erosion models: Sensitivity
740   analysis and intermodel comparison. J Geophys Res B: Solid Earth. 107(B9).

741   Uren J, Price W. 2005. Surveying for engineers. 4th ed. New York: Palgrave Macmillan.

742   Vatne G. 2001. Geometry of englacial water conduits, Austre Brøggerbreen, Svalbard. Norsk
743   Geografisk Tidsskrift. 55(2):85-93.

744   Vatne G, Irvine-Fynn TDL. 2016. Morphological dynamics of an englacial channel. Hydrol Earth
745   Syst Sci. 20(7):2947-2964.

746   Vatne G, Refsnes I. 2003. Channel pattern and geometry of englacial conduits. 6th International
747   Symposium 'Glacier caves and karst in Polar Regions'; Ny-Ålesund, Svalbard. p. 181-188.

748   Whipple KX, Tucker GE. 1999. Dynamics of the stream-power river incision model: Implications for
749   height limits of mountain ranges, landscape response timescales, and research needs. J Geophys Res
750   B: Solid Earth. 104(B8):17661-17674.

751   Whittaker AC, Boulton SJ. 2012. Tectonic and climatic controls on knickpoint retreat rates and
752   landscape response times. J Geophys Res F: Earth Surf. 117(F2).

753   Wilcox AC, Wohl EE. 2006. Flow resistance dynamics in step-pool stream channels: 1. Large woody
754   debris and controls on total resistance. Water Resour Res. 42(5):W05418.

755   Wilcox AC, Wohl EE, Comiti F, Mao L. 2011. Hydraulics, morphology, and energy dissipation in an
756   alpine step-pool channel. Water Resour Res. 47(7):W07514.

757   Willis IC, Arnold NS, Brock BW. 2002. Effect of snowpack removal on energy balance, melt and
758   runoff in a small supraglacial catchment. Hydrol Process. 16(14):2721-2749.

759   Wohl EE. 1998. Bedrock channel morphology in relation to erosional processes. In: Tinkler KJ, Wohl
760   EE, editors. Rivers Over Rock: Fluvial Processes in Bedrock Channels. Washington, D.C.: American
761   Geophysical Union; p. 133-151.

762   Wu S, Rajaratnam N. 1998. Impinging jet and surface flow regimes at drop. J Hydrol Res 36(1):69-
763   74.

764   Yang K, Smith LC, Chu VW, Pitcher LH, Gleason CJ, Rennermalm AK, Li M. 2016. Fluvial

765   morphometry of supraglacial river networks on the southwest Greenland Ice Sheet. GIScience &

766   Remote Sensing. 53(4):459-482.

767   Yokokawa M, Izumi N, Naito K, Parker G, Yamada T, Greve R. 2016. Cyclic steps on ice. J Geophys

768   Res Earth Surf. 121(5):1023-1048.

769   Zimmermann A, Church M. 2001. Channel morphology, gradient profiles and bed stresses during

770   flood in a step–pool channel. Geomorphology. 40(3-4):311-327.

771   **Table 1.** Summary of knickpoint and cross-section dimensions, flow parameters, and general interpolated weather trends for each day.
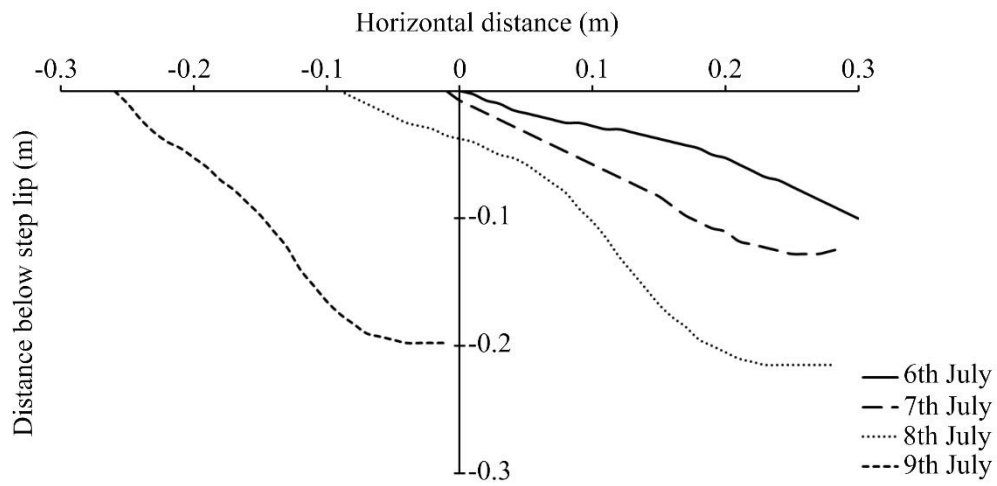
Day	Step height (mm)	Step gradient (°)	Cross-section above knickpoint		Cross-section below knickpoint		Peak discharge ($m^3 s^{-1}$)	Mean velocity ($m\ s^{-1}$)	Maximum stream power per unit length ($W\ m^{-1}$)	Mean water temperature (°C)	Froude number range		Reynolds number range	Mean daily air temperature (°C)	Mean daily potential incident radiation ($W\ m^{-2}$)
			Mean depth (m)	Width (m)	Mean depth (m)	Width (m)					Above knickpoint	Below knickpoint			
6th July	100	18	-	-	-	-	0.013	0.75	46.81	0.3	1.08	0.76	4431	13.85	898
7th July	128	23	0.35	0.29	0.48	0.17	0.011	0.83	47.42	0.17	0.76 - 0.99	0.91 - 0.99	2836 - 6263	12.35	712
8th July	215	30	0.38	0.29	0.55	0.17	0.003	0.41	14.63	0.08	0.2 - 0.69	0.24 - 0.69	1004 - 3131	14.67	768
9th July	198	38	0.46	0.09	0.53	0.25	-	-	-	-	-	-	-	-	-

772

773

Figure 1

775

776

Figure 2

778

779

Figure 3

low discharge

high discharge

enhanced melt from pooling

hydraulic jump

step lip   step-riser   pool

781

Figure 4

6th - 7th July   7th - 8th July   8th - 9th July

0   10 cm   0   10 cm   0   10 cm

————— original

············· end

— — — model

783
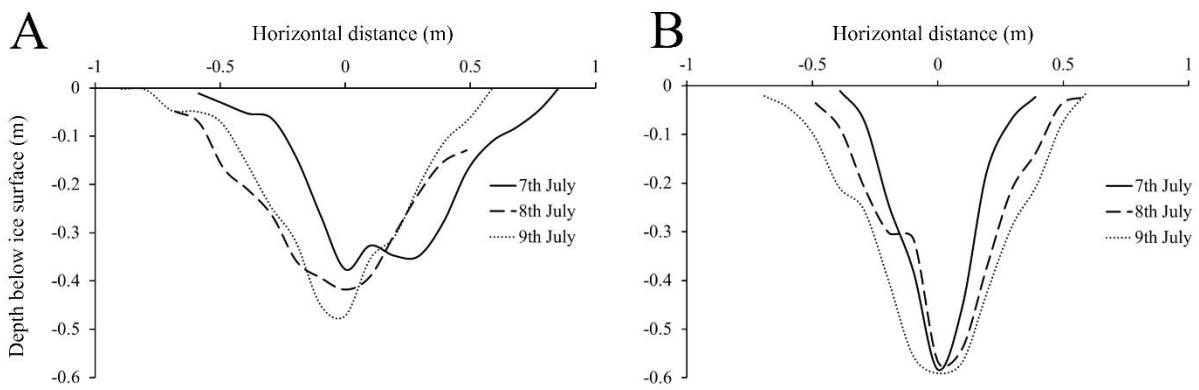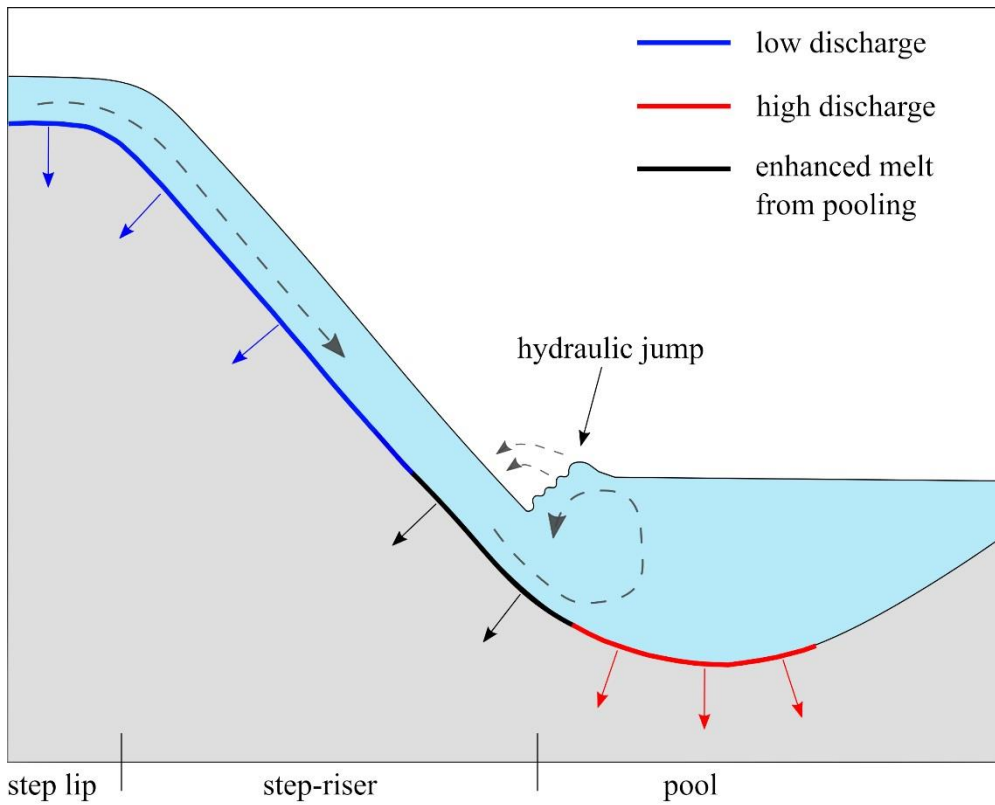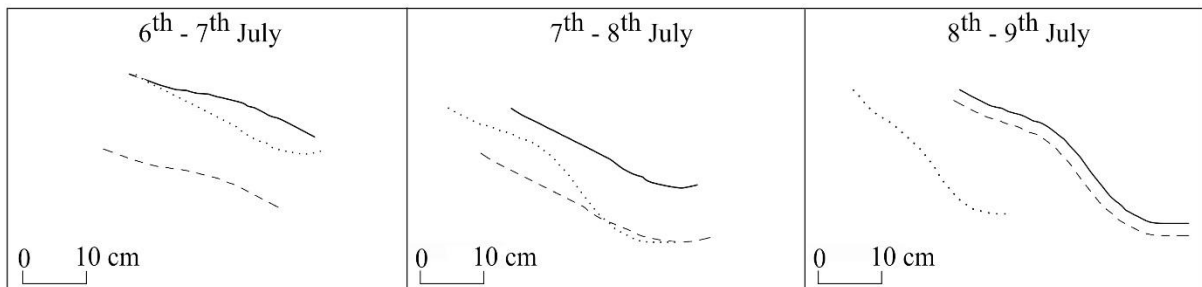
Figure 5.

785

786

787

788

789

Figure 1. (A) The red cross marks the field experiment location on Vadrec del Forno, with the location of the glacier within Switzerland inset. RapidEye imagery obtained from PlanetTeam (2017). (B) The stream reach planform, demonstrating the fracture and undulation troughs upstream of the knickpoint. Longitudinal foliation within the stream vicinity is oriented between 58° and 89° relative to north. Water and glacier flow is also to the north. Aerial imagery obtained from an elevation of 30 m at a resolution of 0.02 m using a DJI Phantom 3 Series Standard quadcopter. (C) The step with the direction of water flow denoted by the black arrow. The 2.3 m long crevasse probe lying horizontal on the far stream bank provides scale. (D) Schematic longitudinal profile of the knickpoint, demonstrating the locations at which cross-section geometry and step height was measured, with an example cross-section inset.

Figure 2. Central step-riser profiles for each day demonstrating the recession and morphology of the step face immediately downstream of the step lip. The graph origin denotes the location of the original step lip (6th July). To facilitate direct comparison, profiles have not been corrected for vertical lowering.

Figure 3. Channel cross-sections measured on different days illustrating changes above (A) and below (B) the knickpoint. The direction of flow is into the page. Cross-sections are geometrically accurate relative to the glacier surface at the time of measurement, with the x-axis denoting lateral distance from the thalweg.

Figure 4. Schematic illustration of the differing zones of erosion across the knickpoint at varying discharges. The solid arrows denote the direction of boundary erosion and the dashed arrows denote the direction of water flow.

Figure 5. Observed and modelled knickpoint evolution for each day, showing the original knickpoint profile (as recorded on the start date), the end profile (as recorded on the end date) and the modelled profile derived from 18-hour melt rates.